A preliminary evaluation of ZSM-5/SBA-15 composite supported Co catalysts for Fischer–Tropsch synthesis

Liy–Yang Wu[a, c]

Zhuo Li[a, *]

lizhuo@qibebt.ac.cn

Dez–Zhi Han[a]

Jinh–Hu Wu[a, b]

Dongk–Ke Zhang[a, b]

[a]Key Laboratory of Biofuels, Qingdao Institute of Bioenergy and Bioprocess Technology, Chinese Academy of Sciences, Qingdao 266101, P–R– China

[b]Centre for Energy (M473), The University of Western Australia, 35 Stirling Highway, Crawley, WA 6008, Australia

[c]University of Chinese Academy of Sciences, Beijing– 100049, P–R– China

*Corresponding author. Tel./fax: + 86 532 8066 2763.

Abstract

A series of ZSM-5/SBA-15 composite supported Co catalysts were prepared and evaluated for the Fischer–Tropsch synthesis (FTS) aimed to maximise the selectivity of C_5–C_{22} hydrocarbons in the product. The composite support was prepared by physically mixing ZSM-5 and SBA-15 of varying proportions and the finished catalysts had a constant Co loading of 15%wtwt.%. The catalysts were tested for their performance in a high pressure fixed-bed reactor operating at T = 240 °C, P = 2.0 MPa, H_2/CO = 2 and GHSV = 1000 h^{-1}. The composite supported catalysts were shown to have much improved catalytic performance over the respective single material supported catalysts. The catalyst with 20%wtwt.% ZSM-5 in the composite support gave the maximum CO conversion (90.6%), maximum selectivity of C_5–C_{22} hydrocarbons (70.0%) and minimum selectivity of light hydrocarbons (13.3% for CH_4 and 7.0% for C_2–C_4 alkanes). The catalysts were characterized using X-ray diffraction, X-ray photoelectron spectroscopy, scanning electron microscopy, transmission electron microscopy with an energy dispersive X-ray spectrometer, temperature programmed desorption and temperature programmed reduction. It was revealed that the superior catalytic performance can be attributed to the large pore size and high dispersion of Co_3O_4, which afforded an optimum reducibility and acid site density.

Keywords: Catalysis; Cobalt; Fischer–Tropsch synthesis; Hydrocarbons; Selectivity; ZSM-5/SBA-15 composite

1 Introduction

The Fischer–Tropsch synthesis (FTS) process is a collection of chemical reactions that converts a mixture of carbon monoxide and hydrogen, also known as syngas, into clean liquid fuels or valuable chemicals [1–4]. Its products are a wide-range of hydrocarbons from CH_4 to heavy molecular weights and can be sulphur- and nitrogen-free with high cetane number fuels, usually following an Anderson–Schulz–Flory distribution [5,6]:

$$W_n/n = (1-\alpha)^2\alpha^{n-1} \quad (1)$$

where W_n is the weight fraction of hydrocarbon molecules containing n carbon atoms and α is the chain growth probability determined by the catalyst and the specific process conditions. It can be explained by the chain growth mechanism of hydrogenation of CO, the hydrogenolysis (cleavage with H_2) of C–O bonds and the formation of C–C bonds. Iron (Fe), cobalt (Co), and ruthenium (Ru) are among the most studied metals in formulating the Fischer–Tropsch catalysts. The high cost of Ru has hindered its industrial-scale application and as such, Ru is often limited to laboratory studies [2,7]. Between Fe and Co, Co-based catalysts for FTS are usually preferred due to their high selectivity in linear paraffin fractions, slow deactivation, less oxygenates and low water–gas shift (WGS) activity [2,8–11]. Although many catalysts have been developed, selectivity control towards gasoline and middle distillate is one of the most important and difficult challenges.

One possible means to control the products is to use the support with controllable pore sizes [2]. The use of periodic mesoporous silicas, for instance, MCM-41 and SBA-15, as supports for preparing Co-based FTS catalysts has been explored [12–15]. The size-controlled pore distribution and high surface area of SBA-15 allows for restricting the formation of hydrocarbons longer than some characteristic size (say, carbon number n < 20), as well as a better control on the cobalt particle size and higher dispersions at higher Co loading as compared to conventional amorphous silica. Martínez et al. [12] studied the influence of cobalt precursor and loading as well as promoters on the catalytic properties of Co/SBA-15 for Fischer–Tropsch synthesis. Catalysts prepared from organic cobalt precursors showed very low FTS activities than those prepared from cobalt nitrate. Xiong et al. [15] investigated the role of pore size in Co/SBA-15 as a FTS catalyst and found that the C_{5+} selectivity increased with increasing the SBA-15 pore size up to 9.32 nm but remained unchanged for larger pore sizes.

It was also well established that the acidic zeolite as a catalyst support or in combination with the conventional support could lead to the enhanced selectivity of gasoline [6,16,17]. Li et al. [18] studied gasoline-range hydrocarbon synthesis with CO_2-containing syngas by using SiO_2/HZSM-5 hybrid-supported Co catalysts. The CO_2 conversion reached the maximum of 20.3% at $CO_2/(CO + CO_2)$ ratio of 0.42. Sartipi et al. [19] introduced mesopores into the structure of HZSM-5 used as support. The Co/mesoH-ZSM-5 showed higher selectivity of the gasoline-range products than Co/H-ZSM-5. However, the activity of catalysts based on mesoH-ZSM-5 decreased quickly in just 30 ~~hrs~~h. The SiO_2/Al_2O_3 ratio and the crystal size of ZSM-5 have a strong effect on the catalytic performance and product selectivity. The strong acidity and long-path micropores usually cause the over-cracking to undesirable light hydrocarbons (CH_4 and C_2–C_4 alkanes) [20].

The present contribution reports a preliminary experimental evaluation of ZSM-5/SBA-15 composite supported cobalt catalysts for FTS. It was expected that the combination of SBA-15 with controlled pore sizes and ZSM-5 with proper acidity would facilitate much improved selectivity of the gasoline and middle distillate range hydrocarbons.

2 Experimental

2.1 Catalyst preparation

SBA-15 was prepared as follows: 4.0 g P123 (EO20PO70EO20, MAV = 5800, Aldrich) was dissolved in 120 mL 2 M HCl with stirring to obtain a clear solution. 8.5 g TEOS (Aldrich) was gradually added into the solution with continuous stirring for 24 h. The mixture was hydrothermally processed to crystallize in a Teflon-lined autoclave at 120 °C for 24 h followed by filtering, washing and drying at room temperature. Calcination of the dried cake was then carried out in an electric oven in air at 550 °C for 6 h.

ZSM-5 (SiO_2/Al_2O_3 = 40) was obtained from Qilu Huaxin Industry Co. Ltd. The composite supports were prepared by physically mixing the SBA-15 with the ZSM-5 in different mass ratios. The prepared composites were denoted as ZS-x, where x = 0, 10, 20, 30, 50, and 100, respectively, representing the percent of ZSM-5 in the composite.

Co/ZS-x catalysts were prepared by incipient wet impregnation [21,22] of the respective ZS-x supports with a desired amount of aqueous cobalt nitrate. The precursors were dried at 120 °C and calcined at 400 °C for 4 h. The content of cobalt in the final catalysts was kept constant at 15~~%wt~~wt.%.

2.2 Catalyst characterization

Surface area and porosity were measured using N_2 adsorption–desorption at – 196 °C on an ASAP-2010 Micromeritics instrument. Prior to a measurement, the sample was degassed at 300 °C for 6 h. The surface area was obtained using the BET method, the micropore volume was calculated using the t-plot method [17] and the mesopore volume was calculated using the BJH method [23].

X-ray diffraction patterns of the catalysts were collected on a Brukers D8 powder X-ray diffractometer with Cu-Kα radiation at a rate of 4° min^{-1} in the range 2θ = 5°–70°. The average crystal size of Co_3O_4 was calculated according to the Scherrer equation at 2θ = 36.9°, and the Co^0 dispersion was also estimated according to the literature [12,17], specifically, it was estimated from "D = 96/d, where D is the % dispersion and d is the particle size of Co^0 in nm which equals 0.75 × d (Co_3O_4)."

The surface concentration and oxidation states of cobalt oxides on the catalysts were determined using X-ray photoelectron spectroscopy (XPS) performed on a Physical Electronics Company Quantum-2000 ~~Scaning~~Scanning ESCA Microprobe spectrometer with a Al Kα monochromatized line (1486.6 eV). All binding energies (BEs) were corrected with reference to the C 1 s (284.6 eV). The morphology of the catalyst samples was investigated using scanning electron microscopy (SEM) with a JEOL JSM-7001 F microscope operated at 10 kV. Transmission electron microscopy (TEM) imaging analysis was carried out using a JEM-2010 microscope operated at 200 kV, equipped with an energy dispersive X-ray spectrometer (EDS) attachment (Oxford INCA Penta FETx3).

The acidity of the catalysts was analysed by using temperature programmed desorption (NH_3-TPD). The sample was pretreated at 300 °C for 2 h in Ar and cooled to 50 °C. After being saturated with NH_3, the sample was purged with Ar to remove the physisorbed NH_3. The TPD measurements of desorbed NH_3 were conducted in flowing Ar from 50 °C to 650 °C at a heating rate of 10 °C min^{-1}. All flow rates of Ar ~~metioned~~mentioned above were set to 40 mL min^{-1}.

The reduction behaviour of the supported cobalt phases was performed in a U-tube quartz cell. It was initially purged with Ar (40 mL min^{-1}) at 300 °C for 1 h and cooled to 50 °C, then exposed to 10% H_2/Ar (40 mL min^{-1}) while the temperature was ramped from 50 °C to 800 °C at a heating rate of 10 °C min^{-1}.

2.3 Catalytic performance test

The FTS reaction was performed in a stainless-steel fixed-bed reactor (d_{int} = 8 mm). A catalyst of ~ 1.0 g (250–400 μm and ~ 1.5 mL in volume) was well mixed with 1.5 mL of quartz particles (250–400 μm) and charged into the reactor to form a ~ 3 mL diluted catalyst bed to avoid the formation of hot spots in the catalyst. The catalyst was then reduced in-situ in a H_2 stream at 50 mL min^{-1} at 450 °C for 6 h. During the FTS reaction tests, the reactant gas mixture composed of $H_2/CO/N_2$ = 6/3/1 (v/v) was introduced into the reactor with the reaction condition of 240 °C, 2 MPa and space velocity (GHSV) of 1000 h^{-1}. The reactor effluent passed through a hot trap and a cold trap to collect the products. The gas effluent was analysed on-line for its composition by using an Agilent 7890 chromatograph equipped with a thermal conductivity detector (TCD) and a flame ionization detectors (FID). Another gas chromatograph (Agilent 7820A) equipped with a DB-1 capillary column was used to analyse the composition of the liquid products. Each experimental run was repeated at least three times and the carbon balance was also estimated as a means of confirming the validity of the experimental runs. It was found that above 90% carbon balance was achieved for all reported experiments.

3 Results and discussion

3.1 Performance of the catalysts in Fischer–Tropsch synthesis

As summarized in Table 1, the composite supported catalysts clearly displayed superior catalytic performance compared to the respective single materials supported catalysts. The composite supported catalysts showed a low selectivity of C_1–C_4 hydrocarbons and high selectivity of C_5–C_{22}. Although the CO conversion was not significantly altered with increasing the ratio of ZSM-5 in the composite up to 20%, the selectivity of the CH_4 and C_2–C_4 hydrocarbons drastically decreased and the selectivity of the C_5–C_{22} range of hydrocarbons was enhanced. Note especially that the selectivity of the middle distillate hydrocarbons C_{12}–C_{22} had increased from 26.6% for Co/ZS-0 to 38.0% for Co/ZS-20. This is believed to be related to the higher cobalt dispersion and larger pore sizes in the catalysts with a higher ratio of ZSM-5 up to 20% (as evidenced by the XRD and BET results in Tables 4 and 3), which benefited the production of long chain hydrocarbons but not the CH_4 and C_2–C_4 hydrocarbons [24]. Meanwhile, the addition of ZSM-5 is also thought to facilitate the cracking of longer chain hydrocarbons to C_5–C_{22}. However, with the further increase in the proportion of ZSM-5, the CO conversion decreased to 87.9% for Co/ZS-30 and 84.9% for Co/ZS-50, accompanied by increased selectivity of CH_4 and C_2–C_4 hydrocarbons and lowered selectivity of C_5–C_{22} hydrocarbons. Compared to the physically mixing of Co/SiO_2 and HZSM-5 reported in the literature [17], the present ZSM-5/SBA-15 composite supported Co catalysts clearly showed a higher selectivity towards C_{12}–C_{22}. For catalyst Co/ZS-100 with only ZSM-5 as the support, however, the CO conversion and selectivity of C_5–C_{22} were only 70.5% and 58.0%, respectively, while the products shifted to heavier hydrocarbons C_{23+} (with a yield as high as 11.6%). Although, due to its high acidity, ZSM-5 has a tendency to crack hydrocarbons to lighter products, the FTS process involves competing reactions of both chain-growth and cracking simultaneously. The low content of alumina (silica/alumina = 36) and large crystal size of Co_3O_4 is thought to favour the formation of long-chain products [25,33]. In the present work, the silica/alumina ratio of ZSM-5 was 40 and the crystal size of Co_3O_4 in the Co/ZS-100 catalyst was estimate to be 26.0 nm, which facilitated more chain-growth than cracking. Thus the C_{12}–C_{22} selectivity was as high as 34.1% and the C_{23+} selectivity was also the highest on the Co/ZS-100 catalyst.

Table 1 The activity and selectivity results for the FTS reaction over the Co/ZS-x series catalysts.

Catalyst	CO conversion (%)	Hydrocarbon selectivity (%)						
		CH_4	C_2–C_4	C_{5+}	C_5–C_{11}	C_{12}–C_{22}	C_5–C_{22}	C_{23+}
Co/ZS-0	90.0	23.4	11.5	65.1	33.9	26.6	60.5	4.7
Co/ZS-10	90.2	21.4	10.0	68.86	33.1	29.3	62.4	6.4
Co/ZS-20	90.6	13.3	7.0	79.7	32.0	38.0	70.0	9.7
Co/ZS-30	87.9	13.8	8.8	77.34	33.6	35.2	68.8	8.5
Co/ZS-50	84.9	18.7	9.4	71.9	34.7	30.7	65.4	6.5
Co/ZS-100	70.5	18.5	12.0	69.65	23.9	34.1	58.0	11.6

Reaction conditions: T = 240 °C, P = 2.0 MPa, H_2/CO = 2 and GHSV = 1000 h^{-1}.

An effort was made to compare the present results against the literature data (as listed in Table 2), albeit the difficulties in finding literature information on the same catalysts and reaction conditions. Nevertheless, the present work generally achieved higher CO conversions. This might be in part due to the lower space velocity employed in the present work. The C_{5+} selectivity was within the range of the literature data. Since the cobalt content in the present catalyst was less than those of the others, the amount of the heavy products was slightly less. It is worthwhile to note that with 20% ZSM-5 in the composite support, the C_{5+} selectivity increased to a level comparable to the literature and more importantly, the yield of the diesel range products (C_{12}–C_{18}) of this work was noticeably higher, indicating some advantages and the synergistic effect of the ZSM-5/SBA-15 composite support [20].

Table 2 A comparison of the present results with the literature data on the FTS reactions.

Sample	Co loading (%)	T (°C)	P (MPa)	SV	H_2/CO	X(CO) (%)	$S(CH_4)$ (%)	$S(C_2–C_4)$ (%)	$S(C_{5+})$ (%)	$S(C_5–C_{11})$ (%)	$S(C_{12}–C_{18})$ (%)	Reference
20CoSBA-n	18.0	220	2.0	13.5 L/g/h	2	23.1	19.5	15.8	64.7	/	/	[12]
Co/SiO_2 + ZSM-5	19.5	250	2.0	13.5 L/g/h	2	45–60	11.0	14.7	74.3	62.2($C_5–C_{12}$)	11($C_{13}–C_{22}$)	[17]
Co/SBA-15	18.1	250	1.0	12.1 L/g/h	2	63.2	22.3	5.7	71.1	/	/	[26]
Co/7SBA_L	20.5 Ru(0.3)	220	2.0	/	2	55	13.5	14.0	72.5	/	/	[27]
Co/11SBA_M	20.8 Ru(0.2)	220	2.0	/	2	55	10.1	9.2	80.8	/	/	[27]
Co/SBA	20	240	2.0	1000 h^{-1}	2	60.82	9.53	6.55	83.92	40.56	27.11	[28]
CoSBA-15	20	235	1.0	16 L/g/h	2	~ 61	17.3	12.5	70.2	44.0($C_5–C_{12}$)	16.8($C_{13}–C_{20}$)	[29]
Co/ZSM5	20	240	2.0	4 L/g/h	2	50.6	24.3	30.8	43.9	43.0($C_5–C_{22}$)	/	[30]
Co/SBA-15-CH	20.1	240	2.0	13.5 L/g/h	1	37.0	5.9	20.6	71.9	/	/	[31]
Co/HZSM-5	20	251	2.0	1500 h^{-1}	2	ca. 50	30.5 ($C_1–C_4$)		69.5	48.5($C_5–C_{12}$)	14.6($C_{13}–C_{18}$)	[32]
Co/ZS-0	15	240	2.0	1000 h^{-1}	2	90.0	23.4	11.5	65.1	33.9	20.6	This work
Co/ZS-20	15	240	2.0	1000 h^{-1}	2	90.6	13.3	7.0	79.7	32.0	29.1	This work
Co/ZS-100	15	240	2.0	1000 h^{-1}	2	70.5	18.5	12.0	69.5	23.9	25.8	This work

3.2 Textural properties of catalysts

Compared with SBA-15 and ZSM-5, the catalysts Co/ZS-0 and Co/ZS-100 showed a decrease in the BET surface area, as shown in Table 3. This could be ascribed to the dilution effect of the supported cobalt oxide phase [31]. The BET surface area, as well as pore volume, had a distinct decrease when more than 20% ZSM-5 was introduced into the support. This was due to the lower BET surface area and pore volume of ZSM-5 as shown in Table 3. While the observed slight increase for Co/ZS-10 and Co/ZS-20 was attributed to the small fraction of ZSM-5 in the support. For Co/ZS-0, SBA-15 pores were clogged by cobalt species that made them inaccessible for nitrogen adsorption. Since the Co/ZSM-5 was prepared by incipient wetness impregnation and the cobalt content was 15~~%wt~~wt.%, the chance for to enter into the micro-pores of ZSM-5 was usually low and CoO_x was most likely to migrate and aggregate on the surface of ZSM-5 [34,35,43]. As a result, the cobalt species did not affect the nitrogen adsorption behaviour of ZSM-5. However, the average surface area and pore volume of the support decreased markedly if more ZSM-5 was added in the support. The presence of SBA-15 and its mesoporous structure favoured the formation of C_{5+} [14]. Note that Co/ZS-20 had the highest pore volume and pore size among all the catalysts. The good performance of Co/ZS-20 can at least be partly attributed to the pore size distribution [36].

Table 3 Textural properties of the samples.

Sample	BET surface area (m^2/g)	Pore volume (cm^3/g)	Micropore volume (cm^3/g)	Mesopore volume (cm^3/g)	Average pore size (nm)
SBA-15	486	0.28	0.04	0.21	2.4
ZSM-5	398	0.16	0.16	0	1.6
Co/ZS-0	382	0.28	0.03	0.15	3.0
Co/ZS-10	396	0.29	0.11	0.16	2.8
Co/ZS-20	387	0.30	0.10	0.17	3.0
Co/ZS-30	316	0.23	0.09	0.12	2.9
Co/ZS-50	309	0.24	0.10	0.12	3.0

Co/ZS-100	273	0.15	0.08	0.05	2.2

3.3 Crystalline phase of catalysts

As shown in Fig. 1, the XRD peaks ascribed to ZSM-5 became more intense with increasing ZSM-5 in the catalyst as expected, while all catalysts showed the presence of well-defined reflection characteristics for Co_3O_4 at 31.3°, 36.8°, 44.8°, 59.4° and 65.2°, indicating the presence of crystalline cobalt species of Co_3O_4 spinel [8]. The nano crystal size thus determined offered an opportunity to examine the effect of nano crystal sizes of the composite ~~mateirals~~materials in catalysis while it is understood that the absolute crystal sizes may not be highly accurate [37]. The trend of the estimated average crystal size of Co_3O_4 and the corresponding Co^0 dispersion with varying amount of ZSM-5 in the catalysts took a volcanic shape with Co/ZS-20 being the smallest crystal size of 12.1 nm and greatest dispersion of 10.6%, as listed in Table 4. The Co_3O_4 crystal sizes in the composite supported catalysts were smaller than in the single SBA-15 and ZSM-5 supported catalysts (14.1 nm for Co/ZS-0 and 26.0 nm for Co/ZS-100). This dispersion trend was also in accordance with the variation trend of CO conversion and the selectivity of C_5–C_{22} for the catalysts. Small crystal sizes and high dispersion of Co_3O_4 in the catalysts play a key role in enhancing the FTS activity [38]. The crystal size of Co_3O_4 in the Co/ZS-100 catalyst (26.0 nm) dramatically exceeded the micropore size of ZSM-5 (0.53 × 0.56 nm, IUPAC), indicating that few Co_3O_4 particles entered the micropores of ZSM-5 and a large fraction of Co_3O_4 located on the external surface of ZSM-5 [35], consistent with the observations in the FTS reactions discussed in the previous section.

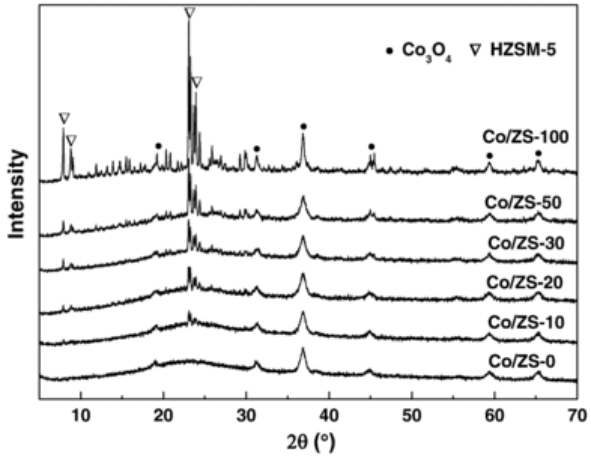

Fig. 1 XRD patterns of the Co/ZS-x series catalysts.

Table 4 The crystal size of Co_3O_4, Co^0 dispersion and surface atomic ratio of Co/Si of the Co/ZS-x series catalysts.

Catalyst	Crystal size of Co_3O_4 (nm)	Co^0 dispersion (%)	Surface atomic ratio (Co/Si)
Co/ZS-0	14.1	9.1	0.034
Co/ZS-10	12.3	10.4	0.047
Co/ZS-20	12.1	10.6	0.075
Co/ZS-30	13.6	9.4	0.051
Co/ZS-50	14.0	9.1	0.072
Co/ZS-100	26.0	4.9	0.401

3.4 XPS characterization of catalysts

The XPS narrow scan spectra for the Co 2p peaks could illustrate the chemical state and surface distribution of the cobalt species. As shown in Fig. 2, the Co $2p_{3/2}$ and Co $2p_{1/2}$ peaks featured at the binding energy (BE) of 780.2–780.8 eV and

795.4–796.1 eV indicate the presence of Co^{2+} or Co^{3+} in the Co_3O_4 spinel phase [35]. Furthermore, for all samples the doublet separation of the binding energy (ΔE) between the Co $2p_{1/2}$ and Co $2p_{3/2}$ peaks was 14.8–15.4 eV, which is close to that of the mixed-valence Co_3O_4 (15.2 eV) [39]. Therefore, Co_3O_4 was considered the predominant cobalt phase in these catalysts after calcination, in agreement with the XRD results. The shallow features (789.3 eV) on the higher energy side of the main peaks could be ascribed to shake-up satellites associated with some Co^{2+} in the high spin state [40], particularly evident for the catalyst Co/ZS-100.

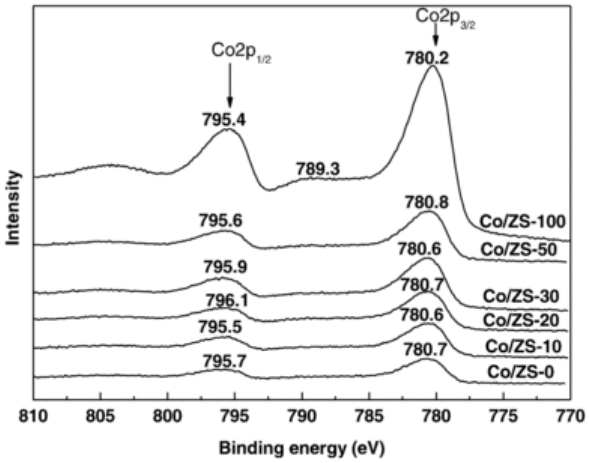

Fig. 2 XPS narrow scan spectra of the Co 2p region for the Co/ZS-x series catalysts.

The peak intensity of Co $2p_{3/2}$ became enhanced with increasing ZSM-5 in Co/ZS-x catalysts, indicating the increased content of Co_3O_4 on the Co/ZS-x catalyst surface. Note that the escape depth of photoelectrons generated during the XPS analysis is less than 10 nm. Compared with Co/ZS-0, the surface atomic ratio of Co/Si increased with increasing ZSM-5 addition but the Co/Si ratio of Co/ZS-100 was 0.401, an order of magnitude higher than those of the other catalysts. It is believed that the cobalt particles were enriched on the exterior surface of the ZSM-5 particles but were distributed on both external and internal surfaces of SBA-15. The disproportional Co/Si ratio relative to the amount of ZSM-5 could have resulted from the different ratio of Co_3O_4 on the external and internal surfaces of the composite support.

3.5 Morphology of catalysts

As can be seen from Fig. 3a and b, Co/ZS-0 (ie. without any ZSM-5 zeolite) consisted of SBA-15 particles of relatively uniform sizes of around 1 μm. The white dots in Fig. 3b were deemed to be the Co_3O_4 particles. The dispersion of the cobalt particles was well distributed. The average crystal size of ZSM-5 in the Co/ZS-100 catalyst was 2–3 μm (Fig. 3d) where the non-uniform small particles observed on the external surface of ZSM-5 were believed to be Co_3O_4. The Co_3O_4 particles observed on ZSM-5 were uneven since some cobalt species agglomerated to large particles. From Fig. 3c, both the SBA-15 structures and the ZSM-5 crystals in the composite can be distinctly observed. The worm-like macrostructures of SBA-15 always aggregated together, and the crystallites of ZSM-5 were distinguished as well.

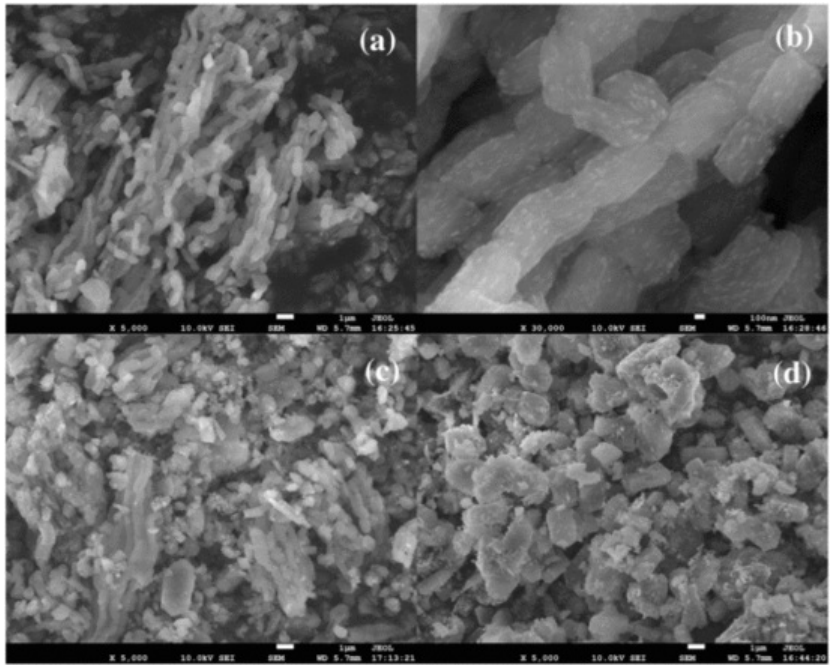

Fig. 3 Typical SEM images of three representative catalyst samples (a) Co/ZS-0; (b) Co/ZS-0 with a larger magnification; and (c) Co/ZS-20; and (d) Co/ZS-100.

It can be directly observed from Fig. 4 that SBA-15 had a highly ordered hexagonal arrangement of the channels and the darker contrasts were representative of Co_3O_4 located both on the external surface and within the channels (Fig. 4a). A similar distribution was also observed on Co/ZS-20 (Fig. 4b), a cross-sectional view of the SBA-15 channels. The pore size in the SBA-15 structure estimated from Fig. 4b was 6.0 nm and the size of cobalt particles inside the SBA-15 channels in Fig. 4a was 5.9 nm. The darkness observed on ZSM-5 (Fig. 4c) was regarded as Co_3O_4 on the external surface of ZSM-5, since the Co signal as well as Si and Al signals were observed from the EDS result (Fig. 4d). It can be speculated that most cobalt particles were likely to form on the external surface of ZSM-5, which was in accord with the SEM image and literature reports that the Co species were prone to migrate and aggregate on the surface of ZSM-5 after the incipient wetness impregnation process with higher cobalt content [35,43].

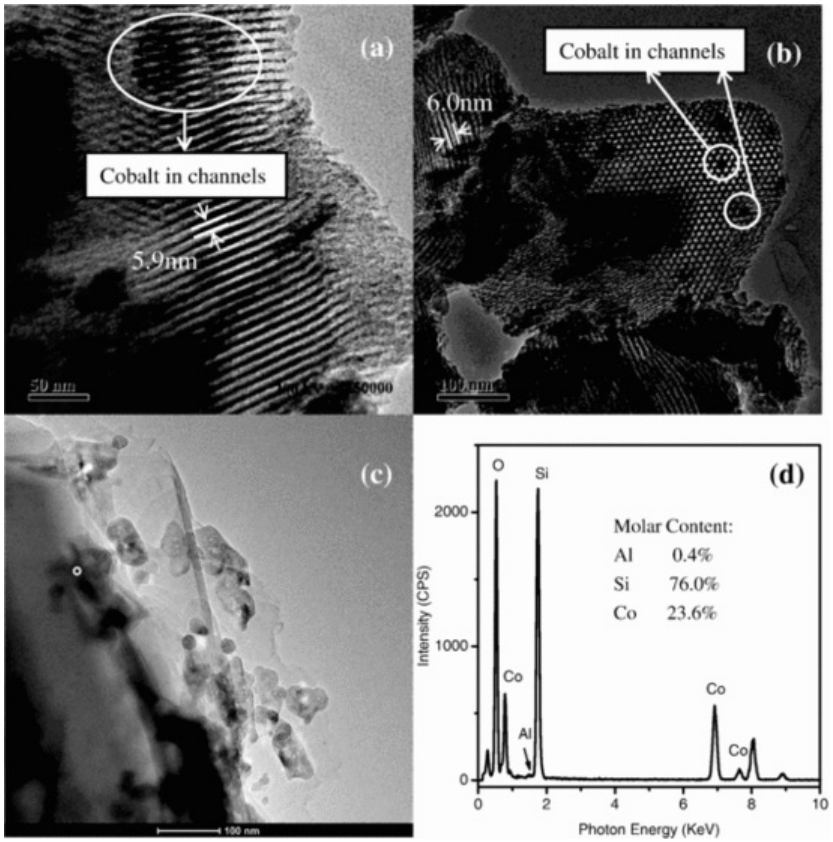

Fig. 4 Typical TEM images of (a) Co/ZS-0; (b) Co/ZS-20; (c) Co/ZS-100; and (d) EDS analysis of point O on Co/ZS-100.

3.6 Acidic properties of catalysts

The surface acidity of an FTS catalyst has a strong impact on the in-situ cracking of products formed [7] and was therefore determined for the present catalysts using NH_3-TPD with results shown in Fig. 5. All the catalysts, including SBA-15, showed a characteristic peak I at about 104 °C, owning to desorption of the physisorbed NH_3 from the Si–OH sites on the surface of SBA-15 or ZSM-5 [41]. The broad peak II at around 486 °C for the single SBA-15 supported catalyst Co/ZS-0 is due to the negligible adsorption of NH_3 on the pure SBA-15 [35], while the peak II at 370 °C for Co/ZS-100 can be assigned to the aluminium centres of ZSM-5 and the dispersion of Co_3O_4 on the support of ZSM-5 [35]. Compared to Co/ZS-0 and Co/ZS-100, peak II for the composite supported catalysts may have originated from the dispersion of Co_3O_4 on the support of SBA-15 and ZSM-5 and the aluminium centres of ZSM-5. It was observed that peak II shifted to lower temperatures with increasing ZSM-5 addition up to 20%wtwt.%, which was in accordance with the literature [35] that the acid strength of the alumina centres of ZSM-5 was less than the dispersion of Co_3O_4 on the support. Peak II shifted to higher temperatures for Co/ZS-30 and Co/ZS-50 than the Co/ZS-20 catalyst, indicating the surface coverage of aluminium centres by the larger crystal sizes of Co_3O_4. Meanwhile, the intensity of the peak above 350 °C was enhanced with increasing the amount of ZSM-5, suggesting the increased acid sites arising from the aluminium centres of ZSM-5 [42]. Table 5 gives the acid site density, expressed as NH_3 adsorbed in mmol per gram of catalyst on Co/ZS catalysts. Generally, the acid site density increased with an increase in the ZSM-5 content in the composite supports. The acid sites could cause the cracking and isomerization of heavier hydrocarbons generated on the surface cobalt sites. However, the acid sites with high strength could also result in the over-cracking to undesired light hydrocarbons (CH_4 and C_2–C_4 alkanes). Co/ZS-20 was found to be the best for the production of middle hydrocarbons, which seems to be consistent with the amount of acid sites on this catalyst.

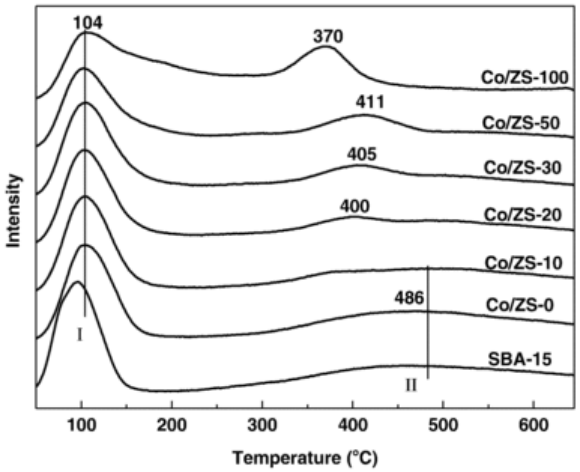

Fig. 5 NH_3-TPD curves of the Co/ZS-x series catalysts.

Table 5 Physicochemical properties of the catalysts.

Catalyst	H_2 consumption below 450 °C (mmol/g)	Overall H_2 consumption (mmol/g)	Degree of reduction (%)[a]	NH_3 uptake (mmol/g)
Co/ZS-0	1.47	2.84	51.8	2.58
Co/ZS-10	1.50	2.84	52.8	2.41
Co/ZS-20	1.34	2.77	48.3	2.63
Co/ZS-30	1.34	2.77	48.4	2.69
Co/ZS-50	1.36	2.58	52.7	2.50
Co/ZS-100	1.83	2.39	76.5	2.90

[a] The degree of reduction is calculated by dividing the H_2 consumption below 450 °C by the total amount of H_2 consumption by the catalysts.

3.7 Reduction behaviour of catalysts

The activity of FTS catalysts strongly depends on the reducibility of the Co_3O_4 species and the H_2-TPR was performed on the present catalysts to assess their reduction behaviour of Co_3O_4. The TPR profiles shown in Fig. 6 allowed the degree of reduction to be estimated by dividing the H_2 consumption below 450 °C by the total H_2 consumption by the catalysts as summarized in Table 5. Fig. 6 shows two distinct reduction peaks, peak I at around 320 °C and peak II at about 450 °C, on the H_2-TPR profiles for the catalysts containing less than 50% ZSM-5. The reduction of Co_3O_4 was a two-step process involving the reduction of Co^{3+} to Co^{2+} at a low temperature and the subsequent reduction of CoO to metallic Co at a high temperature [43]. Therefore, peak I may be attributed to the reduction of Co^{3+} to Co^{2+} and peak II to the reduction of CoO to metallic Co in the present work. The temperature of peak I incurred little alternation (at around 324 °C) while the addition of ZSM-5 in the composite support was increased up to 30%wtwt.%, but was shifted to lower temperatures (at 316 °C and 312 °C) with further addition of ZSM-5 at 50%wtwt.% and 100%wtwt.%. However, the temperature of peak II of the broad profiles comprised of more than one peak was decreased from 460 °C to 445 °C, which is thought to be caused by the coaction of different-sized particles and varying degrees of interaction between the cobalt species and the support [36]. The easy reduction had resulted from the large crystal sizes and the weak interaction between the cobalt species and support. The effect of crystal size of Co_3O_4 was typical for the reduction of CoO to metallic Co (peak II), therefore, the Co/ZS-100 catalyst with the much larger crystal sizes displayed an much easier reduction behaviour at 362 °C, which was in good agreement with the literature reports [12,44]. The degree of reduction for Co/ZS-100 was 76.5%, the highest among the catalysts. The greater extent of reduction facilitated the production of long-chain hydrocarbon products [14]. In addition to the two main reduction peaks, a third peak at around 650 °C (peak III) was also observed for Co/ZS-50 and Co/ZS-100, being more apparent on the latter. This might be caused by the reduction of more stable species, such as cobalt aluminate or cobalt silicate on the ZSM-5 support [45]. The high CH_4 selectivity of FTS over Co/ZS-0 and the large amount of C_{23+} production over Co/ZS-100 were consistent with the literature report [24] that the CH_4 selectivity was enhanced on the CoO surface and the high reducibility of Co_3O_4 was

beneficial to the production of long-chain hydrocarbons.

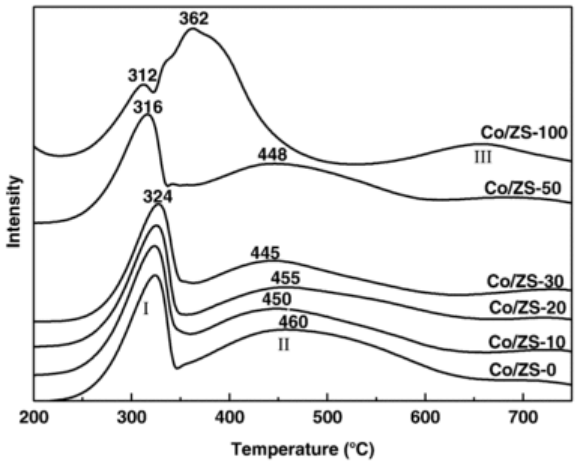

Fig. 6 H_2-TPR profiles of the Co/ZS-x series catalysts.

4 Conclusions

The ZSM-5/SBA-15 composite supported catalysts were shown to have the superior catalytic performance as compared to the single material supported catalysts. The selectivity profiles of the C_1–C_4 and C_5–C_{22} ranges of hydrocarbons took a volcanic shape for the catalysts with increasing amount of ZSM-5 in the support. The catalyst with 20%wtwt.% ZSM-5 in the support shifted the product distribution to the middle distillate range of hydrocarbons, with minimum selectivity of C_1–C_4 and maximum selectivity of C_5–C_{22}. More light hydrocarbons (CH_4 and C_2–C_4 alkanes) were produced with further addition of ZSM-5. The composite support with 20%wtwt.% ZSM-5 showed the optimal amount and strength of acid sites for the cracking of heavier hydrocarbons to C_5–C_{22}.

Acknowledgements

This work was financially supported by the Ministry of Science and Technology of the People's Republic of China (Project No. 2010BAC66B03), Chinese Academy of Sciences (Project No. XDA07070301 and Project No. Y2010022), Entrepreneurial and Innovative Leading Talent Project of Qingdao (13-CX-19) and the Australian Research Council under the ARC Linkage Projects scheme (ARC LP100200136).

References

[1]

J. Kang, S. Zhang, Q. Zhang and Y. Wang, Ruthenium nanoparticles supported on carbon nanotubes as efficient catalysts for selective conversion of synthesis gas to diesel fuel, *Angew. Chem. Int. Ed.* **48**, 2009, 2565–2568.

[2]

Q. Zhang, J. Kang and Y. Wang, Development of novel catalysts for Fischer–Tropsch synthesis: tuning the product selectivity, *ChemCatChem* **2**, 2010, 1030–1058.

[3]

M.E. Dry, High quality diesel via the Fischer–Tropsch process—a review, *J. Chem. Technol. Biotechnol.* **77**, 2002, 43–50.

[4]

M. Stelmachowski and L. Nowicki, Fuel from the synthesis gas—the role of process engineering, *Appl. Energy* **74**, 2003, 85–93.

[5]

D.N. Vo, V. Arcotumapathy, B. Abdullah and A.A. Adesina, Evaluation of Ba-promoted Mo carbide catalyst for Fischer–Tropsch synthesis, *J. Chem. Technol. Biotechnol.* **88**, 2013, 1358–1363.

[6]

X. Liu, A. Hamasaki, T. Honma and M. Tokunaga, Anti-ASF distribution in Fischer–Tropsch synthesis over unsupported cobalt catalysts in a batch slurry phase reactor, *Catal. Today* **175**, 2011, 494–503.

[7]

J. Kang, K. Cheng, L. Zhang, Q. Zhang, J. Ding, W. Hua, Y. Lou, Q. Zhai and Y. Wang, Mesoporous zeolite-supported Ruthenium nanoparticles as highly selective Fischer–Tropsch catalysts for the production of C_5–C_{11} isoparaffins, *Angew. Chem. Int. Ed.* **50**, 2011, 5200–5203.

[8]

L. Yu, X. Liu, Y. Fang, C. Wang and Y. Sun, Highly active Co/SiC catalysts with controllable dispersion and reducibility for Fischer–Tropsch synthesis, *Fuel* **112**, 2013, 483–488.

[9]

M. Dalil, M. Sohrabi and S.J. Royaee, Application of nano-sized cobalt on ZSM-5 zeolite as an active catalyst in Fischer–Tropsch synthesis, *J. Ind. Eng. Chem.* **18**, 2012, 690–696.

[10]

N.S. Hondow, G.A. Koutsantonis, R.O. Fuller, H. Fansuri, M. Saunders, R.L. Stamps and D. Zhang, The modification of M41S materials: addition of metal clusters and nanoparticles, *New J. Chem.* **34**, 2010, 1286–1294.

[11]

M. Khobragade, S. Majhi and K.K. Pant, Effect of K and CeO_2 promoters on the activity of Co/SiO_2 catalyst for liquid fuel production from syngas, *Appl. Energy* **94**, 2012, 385–394.

[12]

A. Martınez, C. López, F. Márquez and I. Dıaz, Fischer–Tropsch synthesis of hydrocarbons over mesoporous Co/SBA-15 catalysts: the influence of metal loading, cobalt precursor, and promoters, *J. Catal.* **220**, 2003, 486–499.

[13]

A.Y. Khodakov, R. Bechara and A. Griboval-Constant, Fischer–Tropsch synthesis over silica supported cobalt catalysts: mesoporous structure versus cobalt surface density, *Appl. Catal. A Gen.* **254**, 2003, 273–288.

[14]

A.Y. Khodakov, A. Griboval-Constant, R. Bechara and V.L. Zholobenko, Pore size effects in Fischer Tropsch synthesis over cobalt-supported mesoporous silicas, *J. Catal.* **206**, 2002, 230–241.

[15]

H. Xiong, Y. Zhang, K. Liew and J. Li, Fischer–Tropsch synthesis: the role of pore size for Co/SBA-15 catalysts, *J. Mol. Catal. A Chem.* **295**, 2008, 68–76.

[16]

F.G. Botes and W. Böhringer, The addition of HZSM-5 to the Fischer–Tropsch process for improved gasoline production, *Appl. Catal. A Gen.* **267**, 2004, 217–225.

[17]

A. Martínez, J. Rollán, M.A. Arribas, H.S. Cerqueira, A.F. Costa and E.F. S.-Aguiar, A detailed study of the activity and deactivation of zeolites in hybrid Co/SiO_2-zeolite Fischer–Tropsch catalysts, *J. Catal.* **249**, 2007, 162–173.

[18]

Y. Li, T. Wang, C. Wu, H. Li, X. Qin and N. Tsubaki, Gasoline-range hydrocarbon synthesis over Co/SiO_2/HZSM-5 catalyst with CO_2-containing syngas, *Fuel Process. Technol.* **91**, 2010, 388–393.

[19]

S. Sartipi, K. Parashar, M.J. Valero-Romero, V.P. Santos, B. van der Linden, M. Makkee, F. Kapteijn and J. Gascon, Hierarchical H-ZSM-5-supported cobalt for the direct synthesis of gasoline-range hydrocarbons from syngas: advantages, limitations, and mechanistic insight, *J. Catal.* **305**, 2013, 179–190.

[20]

Z. Di, C. Yang, X. Jiao, J. Li, J. Wu and D. Zhang, A ZSM-5/MCM-48 based catalyst for methanol to gasoline conversion, *Fuel* **104**, 2013, 878–881.

[21]

Y. Shen, Q. Zhao, X. Li and D. Zhang, Monodisperse $Ca_{0.15}Fe_{2.85}O_4$ microspheres: facile preparation, characterization, and optical properties, *J. Mater. Sci.* **47**, 2012, 3320–3326.

[22]

J. Liu, X. Li, Q. Zhao and D. Zhang, CuO supportd Ce–Ti mixed oxides for low-temperature SCR of NO with propene, *Adv. Mater. Res.* **518–523**, 2012, 2456–2459.

[23]

E.P. Barrett, L.G. Joyner and P.P. Halenda, The determination of pore volume and area distributions in porous substances. I. Computations from nitrogen isotherms, *J. Am. Chem. Soc.* **73**, 1951, 373–380.

[24]

A.R. de la Osa, A. de Lucas, L. Sánchez-Silva, J. Díaz-Maroto, J.L. Valverde and P. Sánchez, Performing the best composition of supported Co/SiC catalyst for selective FTS diesel production, *Fuel* **95**, 2012, 587–598.

[25]

S. Storsæter, B. Tøtdal, J.C. Walmsley, B.S. Tanem and A. Holmen, Characterization of alumina-, silica-, and titania-supported cobalt Fischer–Tropsch catalysts, *J. Catal.* **236**, 2005, 139–152.

[26]

O. González, H. Pérez, P. Navarro, L.C. Almeida, J.G. Pacheco and M. Montes, Use of different mesostructured materials based on silica as cobalt supports for the Fischer–Tropsch synthesis, *Catal. Today* **148**, 2009, 140–147.

[27]

G. Prieto, A. Martínez, R. Murciano and M.A. Arribas, Cobalt supported on morphologically tailored SBA-15 mesostructures: the impact of pore length on metal dispersion and catalytic activity in the Fischer–Tropsch synthesis, *Appl. Catal. A Gen.* **367**, 2009, 146–156.

[28]

L. Jia, L. Jia, D. Li, B. Hou, J. Wang and Y. Sun, Silylated Co/SBA-15 catalysts for Fischer–Tropsch synthesis, *J. Solid State Chem.* **184**, 2011, 488–493.

[29]

Q.Q. Hao, Y.H. Zhao, H.H. Yang, Z.T. Liu and Z.W. Liu, Alumina grafted to SBA-15 in supercritical CO_2 as a support of cobalt for Fischer–Tropsch synthesis, *Energy Fuel* **26**, 2012, 6567–6575.

[30]

S.H. Kang, J.H. Ryu, J.H. Kim, I.H. Jang, A.R. Kim, G.Y. Han, J.W. Bae and K.S. Ha, Role of ZSM5 distribution on Co/SiO_2 Fischer–Tropsch catalyst for the production of C_5–C_{22} hydrocarbons, *Energy Fuel* **26**, 2012, 6061–6069.

[31]

J.J. Rodrigues, F.A.N. Fernandes and M.G.F. Rodrigues, Study of Co/SBA-15 catalysts prepared by microwave and conventional heating methods and application in Fischer–Tropsch synthesis, *Appl. Catal. A Gen.* **468**, 2013, 32–37.

[32]

S. Wang, Q. Yin, J. Guo, B. Ru and L. Zhu, Improved Fischer–Tropsch synthesis for gasoline over Ru, Ni promoted Co/HZSM-5 catalysts, *Fuel* **108**, 2013, 597–603.

[33]

S. Bessell, ZSM-5 as a support for cobalt Fischer–Tropsch catalysts, In: H.E. Curry-Hyde and R.F. Howe, (Eds.), *Studies in Surface Science and Catalysis* **vol. 81**, 1994, Elsevier, 461–466.

[34]

L.B. Pierella, C. Saux, S.C. Caglieri, H.R. Bertorello and P.G. Bercoff, Catalytic activity and magnetic properties of Co–ZSM-5 zeolites prepared by different methods, *Appl. Catal. A Gen.* **347**, 2008, 55–61.

[35]

F. Bin, C. Song, G. Lv, J. Song, X. Cao, H. Pang and K. Wang, Structural characterization and selective catalytic reduction of nitrogen oxides with ammonia: a comparison between Co/ZSM-5 and Co/SBA-15, *J. Phys. Chem. C* **116**, 2012, 26262–26274.

[36]

Ø. Borg, S. Eri, E.A. Blekkan, S. Storsæter, H. Wigum, E. Rytter and A. Holmen, Fischer–Tropsch synthesis over γ-alumina-supported cobalt catalysts: effect of support variables, *J. Catal.* **248**, 2007, 89–100.

[37]

A. Monshi, Modified Scherrer equation to estimate more accurately nano-crystallite size using XRD, *World J. Nano Sci. Eng.* **2**, 2012, 154–160.

[38]

N. Fischer, E. van Steen and M. Claeys, Structure sensitivity of the Fischer–Tropsch activity and selectivity on alumina supported cobalt catalysts, *J. Catal.* **299**, 2013, 67–80.

[39]

J.Y. Luo, M. Meng, X. Li, X.G. Li, Y.Q. Zha, T.D. Hu, Y.N. Xie and J. Zhang, Mesoporous Co_3O_4–CeO_2 and Pd/Co_3O_4–CeO_2 catalysts: synthesis, characterization and mechanistic study of their catalytic properties for low-temperature CO oxidation, *J. Catal.* **254**, 2008, 310–324.

[40]

H. Xiong, Y. Zhang, K. Liew and J. Li, Ruthenium promotion of Co/SBA-15 catalysts with high cobalt loading for Fischer–Tropsch synthesis, *Fuel Process. Technol.* **90**, 2009, 237–246.

[41]

A. Corma, From microporous to mesoporous molecular sieve materials and their use in catalysis, *Chem. Rev.* **97**, 1997, 2373–2420.

[42]

U.V. Mentzel, K.T. Højholt, M.S. Holm, R. Fehrmann and P. Beato, Conversion of methanol to hydrocarbons over conventional and mesoporous H-ZSM-5 and H-Ga-MFI: major differences in deactivation behavior, *Appl. Catal. A Gen.* **417–418**, 2012, 290–297.

[43]

Z. Zhu, G. Lu, Z. Zhang, Y. Guo, Y. Guo and Y. Wang, Highly active and stable Co_3O_4/ZSM-5 catalyst for propane oxidation: effect of the preparation method, *ACS Catal.* **3**, 2013, 1154–1164.

[44]

A.Y. Khodakov, A. Griboval-Constant, R. Bechara and F. Villain, Pore-size control of cobalt dispersion and reducibility in mesoporous silicas, *J. Phys. Chem. B* **105**, 2001, 9805–9811.

[45]

S.H. Kang, J.H. Ryu, J.H. Kim, P.S. Sai Prasad, J. Bae, J.Y. Cheon and K.W. Jun, ZSM-5 supported cobalt catalyst for the direct production of gasoline range hydrocarbons by Fischer–Tropsch synthesis, *Catal. Lett.* **141**, 2011, 1464–1471.

Graphical abstract

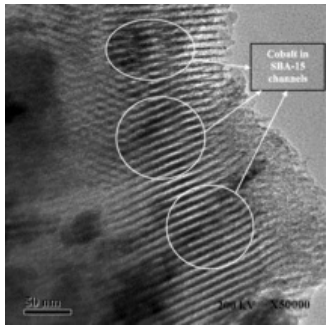

elsevier_FUPROC_4473

Highlights

- ZSM-5/SBA-15 composite supported catalysts showed high C_5^+–C_{22} selectivity.
- Small crystal size and high dispersion of Co species ~~favored~~favoured catalytic activity.
- Optimal reducibility and acid site density benefited middle distillate formation.

Queries and Answers

Query: Your article is registered as a regular item and is being processed for inclusion in a regular issue of the journal. If this is NOT correct and your article belongs to a Special Issue/Collection please contact m.siva@elsevier.com immediately prior to returning your corrections.
Answer: This paper is a regular item.

Query: Please confirm that given names and surnames have been identified correctly.
Answer: All the given names and surnames have been identified and modified correctly.

Query: Would you consider changing the unit “%wt” to “wt.%” in all occurrences in the text? Please check, and amend if necessary.
Answer: I have changed the unit "%wt" to "wt.%" in all occurrences.

Query: The term “mateirals” has been modified to “materials”. Please check if appropriate, and amend if necessary.
Answer: The modified "materials" is appropriate.

Query: Please check the spelling of “supportd” in this reference, and amend if necessary.
Answer: The spelling of "supportd" in the reference is not necessary to amend.